The EMBO Journal (2012) 31, 563–575 | © 2012 European Molecular Biology Organization | All Rights Reserved 0261-4189/12
www.embojournal.org

THE EMBO JOURNAL

H_2O_2 stress-specific regulation of *S. pombe* MAPK Sty1 by mitochondrial protein phosphatase Ptc4

Yujun Di[1], Emily J Holmes[1], Amna Butt[1], Keren Dawson[1], Aleksandr Mironov[2], Vassilios N Kotiadis[3], Campbell W Gourlay[3], Nic Jones[1,*] and Caroline RM Wilkinson[1,*]

[1]Cell Regulation Group, Paterson Institute for Cancer Research, University of Manchester, Manchester, UK, [2]EM Core Facility, Faculty of Life Sciences, University of Manchester, Manchester, UK and [3]Department of Biosciences, University of Kent, Canterbury Kent, UK

In fission yeast, the stress-activated MAP kinase, Sty1, is activated via phosphorylation upon exposure to stress and orchestrates an appropriate response. Its activity is attenuated by either serine/threonine PP2C or tyrosine phosphatases. Here, we found that the PP2C phosphatase, Ptc4, plays an important role in inactivating Sty1 specifically upon oxidative stress. Sty1 activity remains high in a *ptc4* deletion mutant upon H_2O_2 but not under other types of stress. Surprisingly, Ptc4 localizes to the mitochondria and is targeted there by an N-terminal mitochondrial targeting sequence (MTS), which is cleaved upon import. A fraction of Sty1 also localizes to the mitochondria suggesting that Ptc4 attenuates the activity of a mitochondrial pool of this MAPK. Cleavage of the Ptc4 MTS is greatly reduced specifically upon H_2O_2, resulting in the full-length form of the phosphatase; this displays a stronger interaction with Sty1, thus suggesting a novel mechanism by which the negative regulation of MAPK signalling is controlled and providing an explanation for the oxidative stress-specific nature of the regulation of Sty1 by Ptc4.

The EMBO Journal (2012) **31,** 563–575. doi:10.1038/emboj.2011.438; Published online 2 December 2011
Subject Categories: membranes & transport; signal transduction
Keywords: MAP kinase signalling; mitochondria; Ptc4; *S. pombe*; Sty1

Introduction

Cells respond to a broad spectrum of stress conditions in an appropriate and timely manner. Stress-activated MAP kinases (SAPKs) transduce signals induced by environmental changes to downstream effectors such as transcription factors and other signalling proteins which then mediate a response to the stimuli. It is critical that the amplitude and duration of signalling is carefully controlled as perturbations in these parameters can have profound implications for the cell (Kyriakis and Avruch, 2001). This is achieved through the balance between positive and negative regulatory signals as well as through spatial regulation of key components of the signalling network.

There has been remarkable conservation of MAPK signalling pathways throughout evolution. In fission yeast, the stress-activated MAPK Sty1 (also known as Spc1), is homologous to p38, and like its mammalian counterpart, this kinase is activated upon exposure to a wide variety of environmental stimuli, (Millar *et al*, 1995; Shiozaki and Russell, 1995a; Kato *et al*, 1996), whereupon it mediates cellular responses such as changes in transcription and mitotic commitment (Millar *et al*, 1995; Shiozaki and Russell, 1995a; Chen *et al*, 2003; Petersen and Hagan, 2005; Petersen and Nurse, 2007).

Activation of MAPKs occurs through dual phosphorylation of a threonine and tyrosine residue in a Thr-Xxx-Tyr motif within the activation loop; modification of both sites is needed for full activation of the kinase (Payne *et al*, 1991; Robbins *et al*, 1993). Stress-induced activation of Sty1 occurs through phosphorylation of threonine-171 and tyrosine-173 and results in its translocation from the cytoplasm to the nucleus (Gaits *et al*, 1998). Negative regulation of MAPK signalling occurs through removal of these activating phosphate groups. The protein tyrosine phosphatases, Pyp1 and Pyp2 remove tyrosine-173 phosphate (Millar *et al*, 1995; Shiozaki and Russell, 1995a) whereas one of the Ptc enzymes, which are type PP2C serine/threonine phosphatases, acts upon threonine-171 phosphate (Nguyen and Shiozaki, 1999). Some of these phosphatase-encoding genes, such as *pyp1* or *ptc2*, are constitutively expressed whereas others, such as *pyp2* and *ptc1* are stress induced in an Sty1-dependent manner, thereby forming part of a negative feedback loop (Millar *et al*, 1995; Wilkinson *et al*, 1996; Gaits *et al*, 1997). The exact mechanism by which Sty1 is downregulated appears to be context dependent. For instance, basal activity of Sty1 is kept low through the action of Pyp1 whereas Pyp2 is proposed to attenuate Sty1 activity induced upon osmostress (Millar *et al*, 1995; Wilkinson *et al*, 1996) and regulates Sty1's role in nutrient-modulated control of mitotic entry (Petersen and Nurse, 2007). Upon heat shock, Sty1 activation is achieved by abrogation of its interaction with Pyp1 in conjunction with upstream activation of the MAPK pathway, whereas attenuation of heat-induced Sty1 signalling is achieved through the actions of Ptc1 and Ptc3 (Nguyen and Shiozaki, 1999).

Here, we show that another PP2C type phosphatase, Ptc4, plays a major role in regulating Sty1 activation, specifically upon oxidative stress. Intriguingly, Ptc4 resides in the mitochondria suggesting that downregulation of the MAPK is occurring in this organelle. Accordingly, we find a pool of Sty1 in the mitochondria and show that the kinase interacts preferentially with an oxidative stress-specific isoform of Ptc4, which corresponds to the full-length protein. Our data

*Corresponding author. N Jones or CRM Wilkinson, Cell Regulation Group, Paterson Institute for Cancer Research, University of Manchester, Wilmslow Road, Manchester M20 4BX, UK. Tel.: + 44 161 446 3101; Fax: + 44 161 446 3109; E-mail: njones@picr.man.ac.uk or Tel.: + 44 161 446 3129; Fax: + 44 161 446 3109; E-mail: cwilkinson@picr.man.ac.uk

Received: 29 March 2011; accepted: 31 October 2011; published online: 2 December 2011

suggest that the mitochondrial targeting sequence (MTS) of Ptc4, which is usually cleaved upon import of the phosphatase into the mitochondria, acts to promote the interaction of Ptc4 and Sty1 and thus represents a novel means of controlling the negative regulation of MAPK signalling in a stress-specific manner.

Results

Loss of Ptc4 results in prolonged and increased activation of Sty1 upon oxidative stress

We set out to determine how Sty1 activity is attenuated upon oxidative stress. Accordingly, we tested whether Sty1 downregulation was mediated by its known negative regulators, Pyp1, Pyp2 or Ptc1–3. We also tested the potential involvement of another member of the PP2C class, namely Ptc4. Strikingly, Sty1 activation was higher and more prolonged in the *ptc4*Δ mutant upon exposure to H_2O_2 (Figure 1A), but not upon osmotic stress induced by KCl (Figure 1B), $CaCl_2$, NaCl or sorbitol (data not shown). Prolonged exposure of the blots did not reveal elevated levels of Sty1 phosphorylation in the absence of stress, suggesting that Ptc4 does not regulate the basal level of activation of the kinase (data not shown). In contrast, loss of either Pyp2 (Figure 1A) or the combined loss of Ptc1, 2 and 3 resulted in only a modest increase in duration of Sty1 activation (Figure 1C). The basal activity of Sty1 is kept in check through Pyp1 (Shiozaki and Russell, 1995a). Accordingly, we observed higher activation of Sty1 both in the absence of stress and upon H_2O_2 in a *pyp1*Δ mutant but the stress-induced increase in activation of Sty1 was still attenuated upon prolonged exposure to stress (Figure 1D). Ptc4 might affect Sty1 activation directly through dephosphorylation of its phosphor-threonine or alternatively by inactivation of one of the upstream components of the MAPK cascade such as the Wis1 MAPKK or one of the MAPKKKs. To address this, we used a constitutively active form of the MAPKK Wis1, namely *wis1-DD* (Shiozaki *et al*, 1998). If Ptc4 directly dephosphorylates Wis1, or one of the MAPKKKs, then its loss in addition to constitutive activation of Wis1 would not be expected to result in an increase in Sty1 activation above that observed in *wis1-DD* alone (Figure 1E). However, upon exposure to H_2O_2, we observed more Sty1 activity in the *wis1-DDptc4*Δ double mutant compared with *wis1-DD* (Figure 1F and G). These data suggest that Ptc4's ability to regulate Sty1 activation is not dependent upon upstream signalling factors. Consistent with its prolonged activation, Sty1 accumulated in the nucleus with extended kinetics in *ptc4*Δ (Figure 1H). We conclude that Ptc4 plays an important role in downregulating Sty1 activation, specifically upon oxidative stress.

Ptc4 is localized to the mitochondria and exists as an extra isoform upon oxidative stress

As Ptc4 regulated Sty1 specifically upon H_2O_2 stress, we hypothesized that Ptc4 itself might be subject to oxidative stress-specific regulation. Therefore, we examined the Ptc4 protein upon exposure to different stimuli. Under basal conditions, Ptc4 protein migrated as a single isoform with an apparent molecular mass slightly less than predicted. Upon H_2O_2 (Figure 2A and B), but not other stressors (Figure 2B), a second isoform was observed. The appearance of this second isoform was not dependent upon Sty1 (Supplementary Figure S1).

We reasoned that the extra isoform might explain the stress specificity of the *ptc4*Δ phenotype. Examination of the Ptc4 sequence revealed a potential MTS at the N-terminus, as determined by the MitoProt programme (Claros and Vincens, 1996; Figure 2C). Such sequences are often cleaved during translocation of proteins into mitochondria (Habib *et al*, 2007). Therefore, we hypothesized that the upper band might represent the full-length precursor form of Ptc4 with the faster migrating band resulting from cleavage of the putative MTS. This was confirmed by identification of the N-terminal residue of the faster migrating form by Edman degradation (Supplementary Figure S2). Moreover, removal of the MTS resulted in a single isoform of Ptc4 that migrated with the same mobility as wild-type Ptc4 isolated from cells grown in the absence of stress (Figure 5A).

Consistent with the identification of an MTS, Ptc4 colocalized with a known mitochondrial protein, Cox4 (Figure 2D). Upon H_2O_2, Ptc4 still localized to the mitochondria; however, the overall morphology of this organelle had changed (Figure 2E). Instead of a diffuse tubular network, there were two large aggregates at either end of the cell. This is consistent with increased fission which occurs upon exposure to oxidative stress in other organisms (Pletjushkina *et al*, 2006). Prolonged exposure to H_2O_2 led to reformation of a tubular network, presumably as cells adapted to the stimulus (data not shown). The increased fission was slightly delayed in *ptc4*Δ, suggesting that Ptc4 may play a role in regulating mitochondrial morphology (Supplementary Figure S3). In summary, our data show that Ptc4 is localized to the mitochondria whereupon its MTS is cleaved. Upon H_2O_2, cleavage is inhibited resulting in the appearance of the full-length form.

Ptc4 is associated with mitochondrial membranes

We confirmed the localization of Ptc4 to the mitochondria by subcellular fractionation. Ptc4 was found exclusively in the mitochondria but not in the cytoplasm. As observed by immunofluorescence, Ptc4 remained in the mitochondria upon H_2O_2 treatment (Figure 3A). This association persisted upon exposure to high levels of salt, indicating that Ptc4 was not peripherally associated with the cytoplasmic face of the outer mitochondrial membrane (Supplementary Figure S4). Alkali treatment of mitochondria only partially extracted Ptc4, suggesting that it has a strong association with mitochondrial membranes. In contrast, Cox2 was completely resistant to carbonate extraction suggesting that while Ptc4 is strongly attached to mitochondrial membranes, it is not an integral membrane component (Figure 3C). This association was also determined by submitochondrial fractionation (Supplementary Figure S5). Ptc4 does not contain predicted transmembrane regions; thus, we hypothesize that its retention in the membrane fraction is mediated through interactions with integral membrane proteins. Upon stress, only cleaved Ptc4 was extracted by alkali treatment whereas the full-length form was found exclusively in the membrane pellet. This suggested that retention of the MTS promotes the association of Ptc4 with membranes.

To support the idea that Ptc4 was inside mitochondria, we performed a proteinase K protection assay. Upon treatment of mitochondria with protease, Ptc4 was protected, as were known mitochondrial proteins, consistent with Ptc4 being within mitochondria. Both isoforms of Ptc4 were protected in

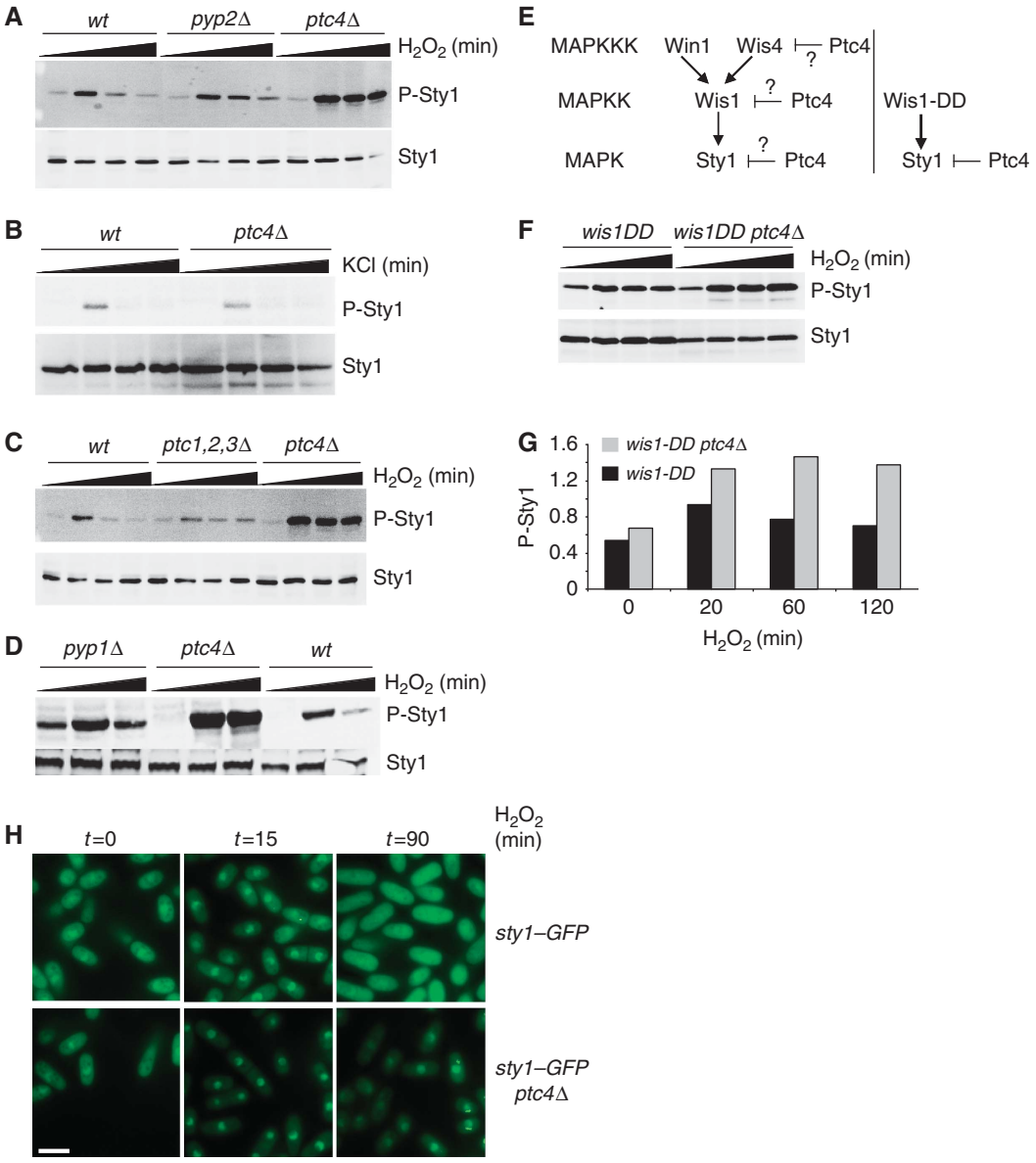

Figure 1 Loss of Ptc4 results in prolonged and increased activation of Sty1 upon oxidative stress. (**A**) Loss of Ptc4 leads to prolonged and increased activation of Sty1 upon treatment with hydrogen peroxide. The indicated strains were grown at 30°C to mid-log phase in YE. Protein samples were prepared before and after treatment with 1 mM H_2O_2 for 30, 120 and 180 min (as indicated by the black triangles) and examined by immunoblotting. Activated Sty1 was detected using anti-phospho p38 antiserum, which recognizes the dually phosphorylated activation site of pTGpY (P-Sty1). Total Sty1 levels (Sty1) were assessed using antiserum raised against Hog1, the *S. cerevisiae* homologue of Sty1. All subsequent experiments have used 1 mM H_2O_2. (**B**) Loss of Ptc4 does not affect Sty1 activation upon osmotic stress. Samples were prepared from cells treated with 0.6 M KCl for 15, 60 and 120 min. (**C**) Sty1 activation was assessed in a *ptc1*Δ,*ptc2*Δ,*ptc3*Δ triple deletion mutant upon exposure to H_2O_2 as in (**A**). (**D**) Sty1 activation was assessed in a *pyp1*Δ mutant upon exposure to H_2O_2 for 15 and 60 min. (**E**) The Sty1 MAPK cascade. The *wis1-DD* allele (right hand panel) encodes a constitutively active form of the Wis1 MAPKK. It has two phospho-mimicking aspartate residues in its activation site at residues 469 and 473, and therefore cannot be activated further by MAPKKK-induced phosphorylation (Shiozaki *et al*, 1998). If Ptc4 were to directly downregulate Wis1 or the kinases upstream (Wis4/Win1), one would not expect to see an increase in Sty1 activation in the *wis1-DDptc4*Δ double mutant compared with *wis1-DD* alone (left hand side). If Ptc4 acts directly upon Sty1, then a *wis1-DDptc4*Δ mutant could potentially display increased Sty1 activity upon H_2O_2. (**F**) Sty1 activation is increased in the *wis1-DDptc4*Δ double mutant compared with *wis1-DD* alone. Extracts were prepared and examined as described in (**A**). Slightly lower levels of Sty1 are observed in the *wis1-DDptc4*Δ mutant compared with *wis1-DD* alone. The reason for this is not clear. (**G**) The densities of the signals corresponding to activated Sty1 were calculated and corrected for the total amount of Sty1. The data shown are representative of three experiments. (**H**) Loss of Ptc4 leads to prolonged accumulation of Sty1 in the nucleus. The indicated strains were grown as described in (**A**) and treated with H_2O_2 before being examined by fluorescence microscopy. The scale bar represents 10 μM. Figure source data can be found in Supplementary data.

a similar manner to the inner mitochondrial membrane protein, Cox2 (Figure 3D), suggesting that both forms have some association with the inner membrane. Treatment of mitochondria with both detergent and protease led to degradation of Ptc4, indicating that its protection was due to its mitochondrial sublocalization and not to inherent resistance to protease (Supplementary Figure S6).

The full-length isoform of Ptc4 might result from oxidation of the phosphatase itself preventing the processing of its MTS. Alternatively, H_2O_2 might modulate other mitochondrial

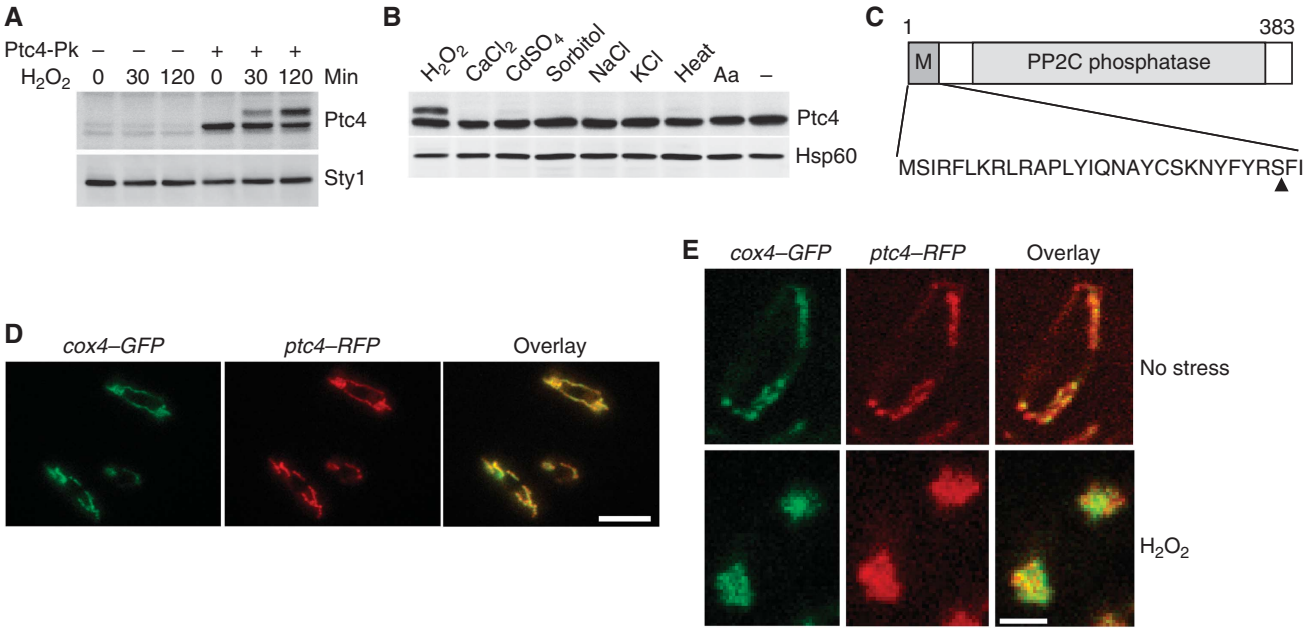

Figure 2 Ptc4 is localized to the mitochondria and exists as an additional isoform specifically upon oxidative stress. (**A**) *ptc4-3Pk* and an untagged control strain were grown to mid-log phase then treated with H_2O_2. Whole cell extracts were examined by immunoblotting with antiserum directed against the Pk epitope to detect Ptc4. Loading was assessed using anti-Hog1 anti serum to detect Sty1. (**B**) Ptc4 protein is modified in an H_2O_2-specific manner. *ptc4-3Pk* was grown to mid-log phase and treated with either 1 mM H_2O_2, 100 mM $CaCl_2$, 0.25 mM $CdSO_4$, 1.2 M sorbitol, 200 mM NaCl, 42°C or 5 μg/ml antimycin A (Aa) for 60 min. Whole cell extracts were examined by immunoblotting with anti-Pk to detect Ptc4 or anti-Hsp60 as a loading control. (**C**) Diagram of the Ptc4 protein (383 amino acids long) showing the putative mitochondrial targeting sequence (MTS), the PP2C phosphatase domain (PP2C) and the cleavage point, indicated by an arrowhead and determined by Edman degradation, which is between residues 28 and 29. (**D**) Colocalization of Ptc4 with a known inner mitochondrial membrane protein, the cytochrome c oxidase subunit, Cox4. The *cox4-GFP ptc4-RFP* strain was examined by immunofluorescence and the GFP and RFP signals overlaid. The scale bar represents 10 μM. (**E**) Ptc4 remains localized to the mitochondria upon H_2O_2 treatment although the mitochondrial morphology changes dramatically. The *cox4-GFP ptc4-RFP* strain was examined by immunofluorescence after 60 min of H_2O_2 treatment. One cell is shown in each panel. The scale bar represents 5 μM. Figure source data can be found in Supplementary data.

Figure 3 A fraction of Sty1 localizes to mitochondria and both Ptc4 and Sty1 associate with mitochondrial membranes. (**A**) Subcellular fractionation was carried out using the *ptc4-3Pk* strain grown in the absence or presence of H_2O_2 for 15 min. Total whole cell extracts were separated by centrifugation into a post-nuclear fraction containing cytoplasm and mitochondria. Further centrifugation resulted in a mitochondrial fraction (M) and the supernatant which consisted of the cytoplasm (C). The resulting mitochondrial fraction was further purified by centrifugation through a sucrose gradient (M*). For the mitochondrial fractions, protein corresponding to 10 times the equivalent cell volume of the cytoplasmic fractions has been loaded. The purity of the fractions was examined by immunoblotting using either anti-Pk antiserum to recognize Ptc4, anti-Hog1 to detect Sty1 or anti-sera to detect the mitochondrial matrix protein Hsp60, the cytoplasmic protein Tpx1 or the nuclear and cytoplasmic protein Rpb1. The Pk antiserum also recognizes two bands, which do not correspond to Ptc4 (see also Figure 2A). These migrate slightly above and below the mature form of Ptc4, and can be seen especially in the cytoplasmic fractions. They are indicated by asterisks. (**B**) Sty1 is hyperactivated in mitochondria isolated from *ptc4*Δ. Mitochondria were purified from the indicated strains in the presence or absence of 1 mM H_2O_2. The time points of stress were 30 min and 2 h. The activation status of Sty1 was assessed by immunoblotting. The results are representative of three independent experiments. (**C**) Association of Ptc4 and Sty1 with mitochondrial membranes. Mitochondria were purified from *ptc4-3Pk* cells grown in the presence or absence of H_2O_2 for 15 min. They were treated with 100 mM sodium carbonate (pH 11) to disrupt both inner and outer mitochondrial membranes and release proteins that are peripherally associated with these structures; these proteins appear in the supernatant fractions (S). Proteins still associated with membranes appear in the pellet (P). Mitochondria were also treated with 100 mM sodium chloride to act as a control demonstrating that protein release with carbonate was due to high pH and not due to the concentration of sodium ions. The fractions of S and P loaded were equivalent to equal volumes of purified mitochondria and were assessed by immunoblotting. (**D**) Proteinase K treatment of purified mitochondria. Mitochondria were prepared from cells treated with and without H_2O_2 for 120 min. The mitochondrial fractions were treated with increasing amounts of proteinase K (PK), 1.25, 2.5 and 5 μg/ml for 30 min (as indicated by the black triangles) and samples examined by immunoblotting. Total represents intact mitochondria; swollen represents mitochondria that were treated with hypotonic buffer to rupture the outer membrane and release the contents of the inner membrane space; sonicated represents the resulting mitoplasts that have been sonicated in the presence of salt which will disrupt the inner membrane to release the matrix contents (such as Hsp60). Cox2 is an inner mitochondrial membrane protein. (**E**) Ptc4 is imported into purified mitochondria *in vitro* but appearance of the cleaved form is reduced upon treatment of mitochondria with H_2O_2. Mitochondria were purified from wild-type *S. pombe* cells that had been treated with 1 mM H_2O_2 for 120 min, Mito (+), or non-treated cells, Mito (−). GST–Ptc4-3Pk was expressed in and purified from *E. coli* and the full-length Ptc4-3Pk protein was released from GST by thrombin cleavage. After incubation with mitochondria, any Ptc4 that had not been imported was degraded by the addition of proteinase K. Ptc4 is not inherently resistant to proteinase K as demonstrated by complete loss of Ptc4 protein upon mixing Ptc4 with proteinase K (compare lanes 6 and 7). FL = full-length Ptc4, M = mature form of Ptc4 which lacks the MTS. The addition of equal amounts of mitochondria to each reaction was assessed using anti-Hsp60 antiserum. Lane 5 contained molecular mass markers which cross-react with the anti-Hsp60 antiserum (indicated by an asterisk). (**F**) EM localization of Sty1 to mitochondria. Immunogold staining of a section through purified mitochondria from wild-type (left hand side) and *sty1-13myc* cells (right hand side) using antibodies to the myc epitope. Secondary antibodies were conjugated to 10 nm colloidal gold. The scale bars represent 200 nM. Figure source data can be found in Supplementary data.

components such that the cleavage of the Ptc4 targeting sequence is now inhibited. To try to distinguish between these possibilities, the import of Ptc4 into mitochondria was recapitulated *in vitro*. Recombinant Ptc4 was imported into purified mitochondria and cleavage to generate the mature form was observed, albeit to a reduced extent compared with its *in-vivo* counterpart (Figure 3E, lane 1). In contrast, when mitochondria were purified from cells treated with H_2O_2, the cleavage of imported recombinant Ptc4 was reduced (Figure 3E, compare the amount of mature Ptc4 in lanes 2 and 4).

In summary, our data indicate that Ptc4 is imported into mitochondria where it has a strong association with mitochondrial membranes. Upon oxidative stress, Ptc4 is still imported but is no longer cleaved due to effect(s) upon the mitochondria and not to some direct modulation of Ptc4 itself.

A fraction of the Sty1 MAPK is also localized to the mitochondria

Immunofluorescence microscopy has indicated that Sty1 is localized to the cytoplasm and accumulates in the nucleus upon stress (Gaits *et al*, 1998; Figure 1H). However, we hypothesized that there may be an additional pool of Sty1 localized to the mitochondria and that this fraction might be downregulated by Ptc4 upon H_2O_2. Indeed, a portion of Sty1 protein co-fractionated with mitochondria (Figure 3A; Supplementary Figure S7). We could detect Sty1 in mitochondria in both the absence and presence of H_2O_2. Consistent with regulation by Ptc4, this mitochondrial pool of Sty1 was hyperactivated in a *ptc4*Δ mutant (Figure 3B). We did not observe a strong activation of Sty1 in wild-type mitochondria but we believe this is due to the methods used for subcellular fractionation, which entail digestion of the cell wall such that cells are not lysed until 90 min after the initial stress imposition whereupon the response to H_2O_2 will be mostly attenuated. Consistent with regulation by Ptc4, this mitochondrial pool of Sty1 was hyperactivated in a *ptc4*Δ mutant (Figure 3B).

Sty1 was not peripherally associated with the cytoplasmic face of the outer mitochondrial membrane (Supplementary Figure S4), but instead was found associated predominantly with the mitochondrial membrane fractions, both in the absence and presence of stress (Figure 3C). Sty1 was protected in the proteinase K assay, in a similar manner to

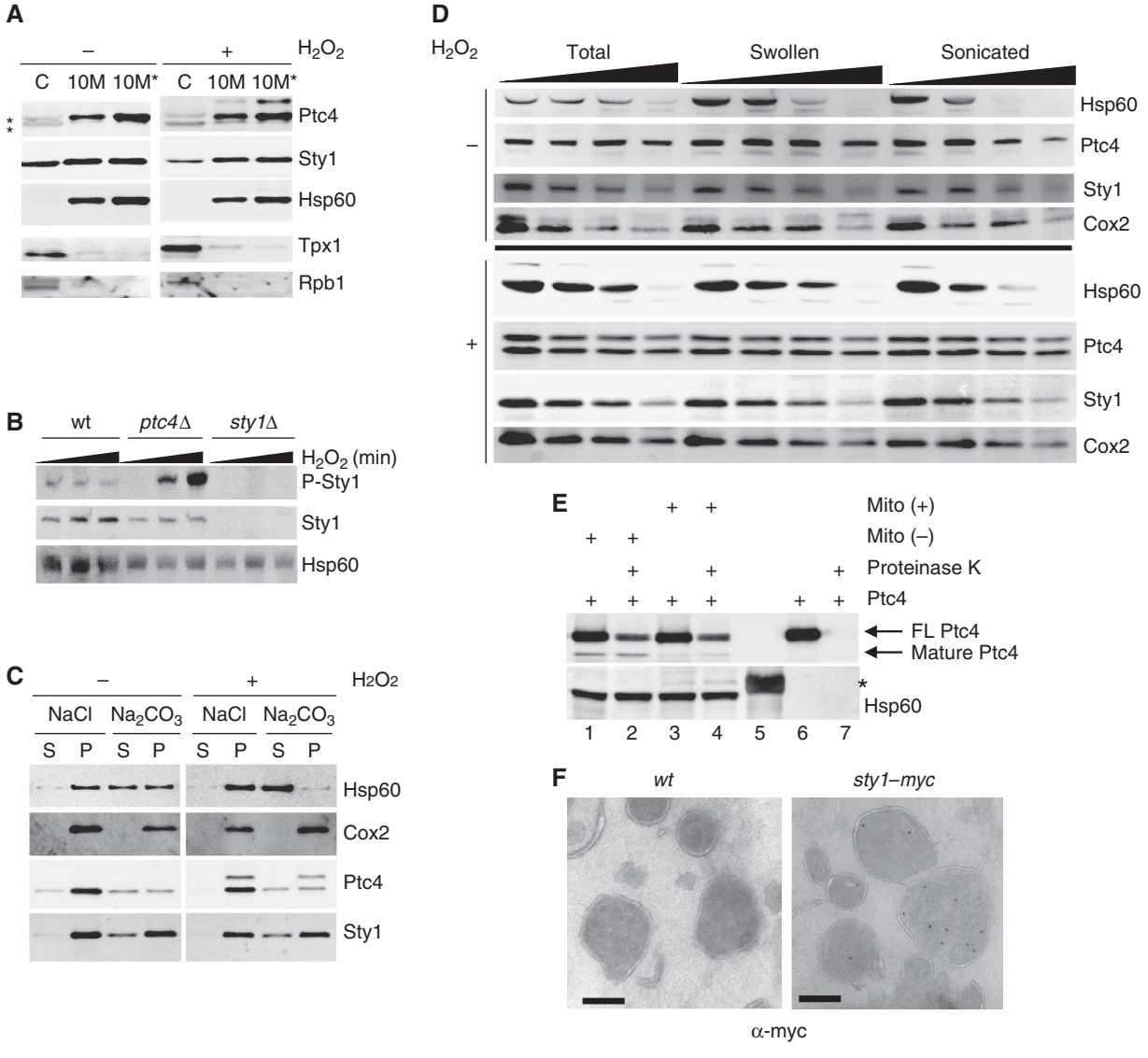

Ptc4 and Cox2 (Figure 3D) suggesting that Sty1 was also associated with the inner membrane. Furthermore, Sty1 was protected to the same extent in the presence or absence of stress, suggesting that it is localized in the same manner under both conditions. The mitochondrial localization of Sty1 was further confirmed by immunoelectron microscopy. Ultrathin sections were prepared from fixed mitochondria and subsequently incubated with antiserum against the myc epitope. Sty1 was localized to the mitochondria by immunogold staining of mitochondria purified from a *sty1-myc* strain (Figure 3F, right hand panel). In contrast, no specific signal was observed in wild-type cells, which contained endogenous untagged Sty1 (Figure 3F, left hand panel). The pattern of labelling suggested that Sty1 is localized within mitochondria as opposed to being associated with the outer membrane. This is in agreement with the fact that mitochondrial Sty1 is afforded protection against degradation by proteinase K (Figure 3D). Taken together, our data indicate that both Ptc4 and Sty1 can be found inside the mitochondria and in particular are associated with components of the inner mitochondrial membrane.

Sty1 interacts preferentially with the full-length isoform of Ptc4

The colocalization of Ptc4 and a proportion of Sty1 suggested that Ptc4 might directly dephosphorylate the mitochondrial pool of Sty1. If this were so, we might expect to detect an interaction between the two proteins. To test this, we performed immunoprecipitation of Ptc4. This resulted in the co-precipitation of Sty1 specifically upon exposure to oxidative stress (Figure 4A, compare lanes 3 and 4). In this case, both isoforms of Ptc4 were precipitated (albeit with only a small fraction of the upper isoform recovered—this is something we consistently see. We do not understand the reason for this but suggest it may be related to the mitochondrial morphological changes that we observe upon stress. It could be that different complexes are formed, or conformational changes occur in Ptc4 that preclude access to the epitope tag). Since the difference between the two conditions was the presence of the Ptc4 precursor, this suggested that the full-length isoform might have greater affinity for Sty1 than the cleaved form. To examine this further, we generated a mutant form of Ptc4, whereby cleavage of the MTS was inhibited. This was achieved by mutating arginines at positions 8, 10 and 27, to alanines. Such basic residues are known to be important for recognition by mitochondrial proteases (Hendrick *et al*, 1989). Accordingly, Ptc4R8A,R10A,R27A was primarily full length (Figure 4A, compare lanes 3 and 5). Although more of this mutant form of Ptc4 was immunoprecipitated than the wild-type full-length protein upon stress, Sty1 was no longer bound. This was the case in either the absence or presence of stress (compare lane 4 with 5 and 6). We hypothesized that if the MTS was important for interacting with Sty1 then mutating the arginines may have interfered with binding between the two proteins. Indeed, the MTS is rich in basic and hydrophobic amino acids, which are characteristic of docking domain motifs known to be responsible for mediating the interactions between MAPKs and other proteins (Sharrocks *et al*, 2000; Supplementary Figure S8).

To test this, we performed an *in-vitro* binding assay. Ptc4 was synthesized *in vitro* and mixed with recombinant GST–Sty1. Some cleavage was apparent in this system as we observed two isoforms of Ptc4 (Figure 4B, upper). Ptc4

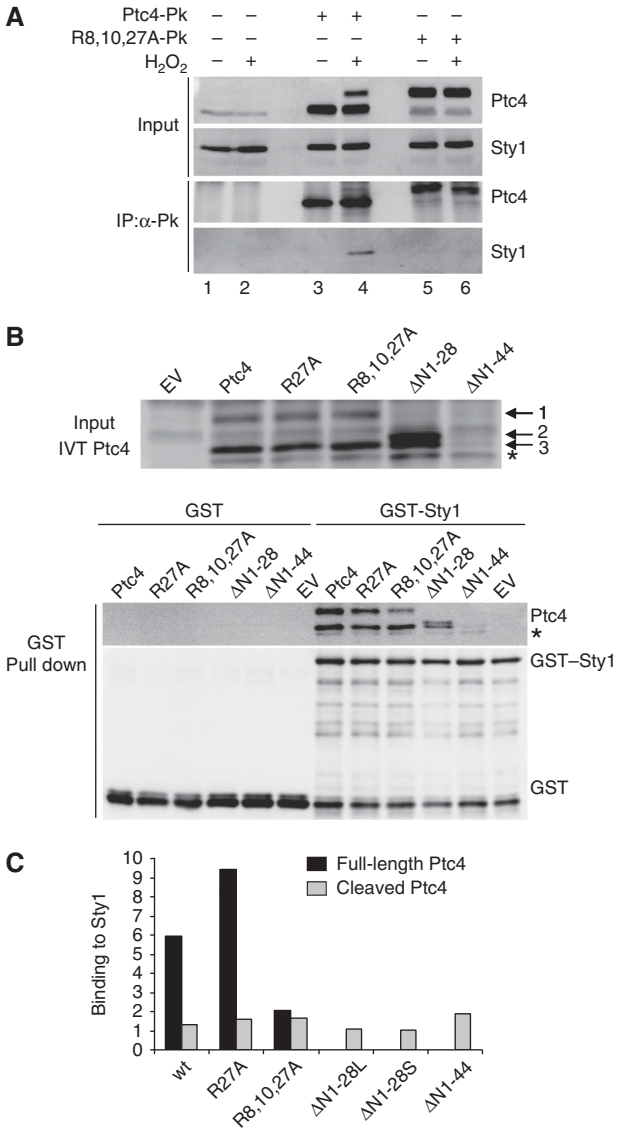

Figure 4 Sty1 preferentially binds to the full-length form of Ptc4. (**A**) Sty1 and Ptc4 interact *in vivo*. Ptc4 was immunoprecipitated using anti-V5 agarose from protein extracts prepared from the following strains: *wild type*, *ptc4-3Pk* or *ptc4R8A,R10A,R27A-3Pk* (R8,10,27A-Pk). Cells were stressed by the addition of H_2O_2 for 30 min as indicated. Whole cell extracts (input) and immunoprecipitated proteins (IP:α-Pk) were analysed by immunoblotting. Ptc4 and Sty1 were detected with anti-Pk and anti-Hog1 antiserum, respectively. Results are representative of three independent experiments. (**B**) Ptc4 and Sty1 interact *in vitro*. Top panel: *in-vitro* translation of Ptc4-3Pk in reticulocyte lysates. Wild-type or various mutant forms were synthesized and examined by western blotting. Ptc4 was detected using anti-Pk antiserum. EV represents *in-vitro* translation reactions using an empty vector. The asterisk indicates a Ptc4 product that is generated from an internal start site, presumably at methionine 45. Band 1 is the full-length form of Ptc4; band 3 is a processed form that lacks the MTS and probably arises from cleavage by proteases present in the reticulocyte lysate; we do not know what form of Ptc4 band 2 represents. Lower panel: GST or GST–Sty1 was expressed in *E. coli*. The purified proteins were mixed with *in-vitro* translated Ptc4. The GST proteins were then precipitated on glutathione sepharose and the amount of Ptc4 bound to Sty1 was assessed by western blotting. (**C**) Ptc4 binding to Sty1 was calculated from (**B**) by comparing the intensity of the signal of Ptc4 bound to Sty1 with the intensity of the Ptc4 input band. The amount of binding was corrected for the amount of GST–Sty1 precipitated in each case. The results are representative of three independent experiments. ΔN1-28L and ΔN1-28S refer to the upper and lower bands, respectively. The black and grey bars represent the Sty1-binding ability of the full-length and cleaved isoforms of Ptc4, respectively. Figure source data can be found in Supplementary data.

co-precipitated with GST–Sty1 but not with GST alone (Figure 4B, lower). Although there was much less full-length Ptc4 in the input, similar amounts of cleaved and uncleaved Ptc4 bound to GST–Sty1 consistent with the full-length form having a much greater affinity for Sty1 (Figure 4C). These data suggest that upon H_2O_2, downregulation of the mitochondrial pool of Sty1 occurs through dephosphorylation by full-length Ptc4. This isoform of Ptc4 is only present upon H_2O_2, due to inhibition of its processing under these conditions thus providing a mechanism to explain the stress-specific nature of this regulation.

Mutating the MTS of Ptc4 disrupts binding to Sty1 and leads to increased activation of the kinase upon oxidative stress

Given that mutating the MTS of Ptc4 abrogated its binding to Sty1, we predicted that downregulation of Sty1 activity upon H_2O_2 should be disrupted in this mutant. Indeed, Sty1 activation remained high in *ptc4R8A,R10A,R27A* upon H_2O_2 compared with wild type (Figure 5A and B), consistent with an intact MTS region being important for attenuation of Sty1 activation. In contrast, the single R27A mutant form of Ptc4, while mostly full length, bound efficiently to Sty1 and displayed normal attenuation of its activation (Figures 4B, C, 5A and B). The double-mutant form, Ptc4R8A,R10A, which has mutations in the putative docking domain, also downregulated Sty1 in a manner comparable to wild type (Figure 5A and B). Only mutation of all three arginines resulted in an inability to reduce activation (Figure 5A and B) and accordingly abrogated binding to Sty1 (Figure 4). These data suggested that there may be redundant docking motifs in this region. Despite disruption to its MTS, Ptc4R8A,R10A,R27A still localized to mitochondria (Figure 5C) and displayed an association with the mitochondrial membrane fraction (Figure 5D). Consistent with the MTS promoting a stronger association with mitochondrial membranes (Figure 3C), neither Ptc4R27A nor Ptc4R8A, R10A,R27A, both of which are predominantly full-length proteins, were extracted by alkali from purified mitochondria (Figure 5D). The importance of the MTS to the correct intracellular localization of Ptc4 was demonstrated by its complete removal (Ptc4NΔ1–28), which prevented localization of Ptc4 to the mitochondria (Figure 5C) and resulted in high levels of Sty1 activation upon H_2O_2 (Figure 5A and B).

Loss of Ptc4 may affect Sty1 directly through loss of dephosphorylation and also indirectly due to disruption of other mitochondrial functions of Ptc4

One possible consequence of hyperactive Sty1 in *ptc4*Δ is that it might provide resistance to H_2O_2. However, the *ptc4*Δ mutant was in fact sensitive to growth when exposed to this stress (Figure 6A). This phenotype is shared by a number of yeast mutants which have defects in controlling respiration (Thorpe *et al*, 2004; Zuin *et al*, 2008), suggesting that Ptc4 might also regulate this process. Accordingly, both *ptc4*Δ and *ptc4NΔ1–28* were unable to grow on either glycerol (Figure 6A) or ethanol (data not shown), both of which are non-fermentable carbon sources. These data suggested that Ptc4 controls the ability of cells to produce energy by oxidative phosphorylation, potentially by regulation of particular mitochondrial target(s). This was supported by an inability of *ptc4*Δ to reduce 2,3,4-triphenyltetrazolium chloride (Figure 6B). In contrast, the triple mutant behaved as wild type on glycerol and in the TTC assay. In order to explore these defects in a more quantitative manner, we carried out high-resolution respirometry. By measuring changes in oxygen concentration in a sealed system, oxygen consumption, which occurs at cytochrome c oxidase (complex IV), can be determined which provides a direct measure of electron transport system activity. The *ptc4*Δ mutant displayed a negligible uptake of oxygen consistent with a complete inability to respire. In contrast, the triple arginine mutant was still able to respire, albeit in a compromised manner (Figure 6C), but this reduced activity was still sufficient to promote growth on non-fermentable carbon sources. The ability of the triple mutant to reduce TTC suggests that the dehydrogenases of the electron transport chain (ETC) are still intact (Figure 6B). In conclusion, Ptc4 is required for ETC activity. Mutating the MTS disrupts the interaction with Sty1 but not the ability of Ptc4 to localize to mitochondria. However, the triple mutant does not behave completely as wild type as respiration is compromised, though not sufficiently to abolish respiratory growth.

Although Sty1 activation remained high in the triple arginine mutant, the kinase did not remain in the nucleus to the same extent as it did in *ptc4*Δ (Figure 6D).

Based on these results, we hypothesize that loss of Ptc4 may affect the Sty1 pathway in more than one way: through direct loss of dephosphorylation of Sty1 and indirectly because of disruption of other mitochondrial-associated functions of Ptc4. In both *ptc4*Δ and the triple mutant, Sty1 activation in the mitochondria was higher than in wild type upon H_2O_2, consistent with direct downregulation by the phosphatase (Figure 5E). The prolonged nuclear accumulation of Sty1 observed in *ptc4*Δ could be due to additional cellular stress caused by mitochondrial defects associated with loss of Ptc4 such as a reduction in oxidative phosphorylation. These effects are not as apparent in the triple mutant, which can still respire sufficiently to allow growth on a non-fermentable carbon source.

Interestingly, the *sty1*Δ mutant also displayed a reduced respiratory capacity suggesting that a possible role for mitochondrial Sty1 is to regulate this activity (Figure 6C).

In summary, the MTS of Ptc4 is essential for targeting the phosphatase to mitochondria and for the interaction with and downregulation of activated Sty1 upon oxidative stress. Within this region, arginine-27 is especially important for promoting cleavage while interaction with Sty1 is facilitated by a combination of arginines 8, 10 and 27. Upon oxidative stress, retention of the MTS promotes association of Ptc4 with the mitochondrial membrane fraction, which is where the mitochondrial pool of Sty1 is preferentially localized.

Discussion

We have demonstrated that Ptc4 belongs to a subset of PP2C phosphatases that reside solely in the mitochondria (Krause-Buchholz *et al*, 2006; Lu *et al*, 2007; Tal *et al*, 2007; Juneau *et al*, 2009). This phosphatase was previously proposed to exist in the vacuole (Gaits and Russell, 1999); however, this conclusion was based on localization of an overexpressed, N-terminally tagged version of the protein, which most likely explains the discrepancy between that finding and this report. Based on the following evidence,

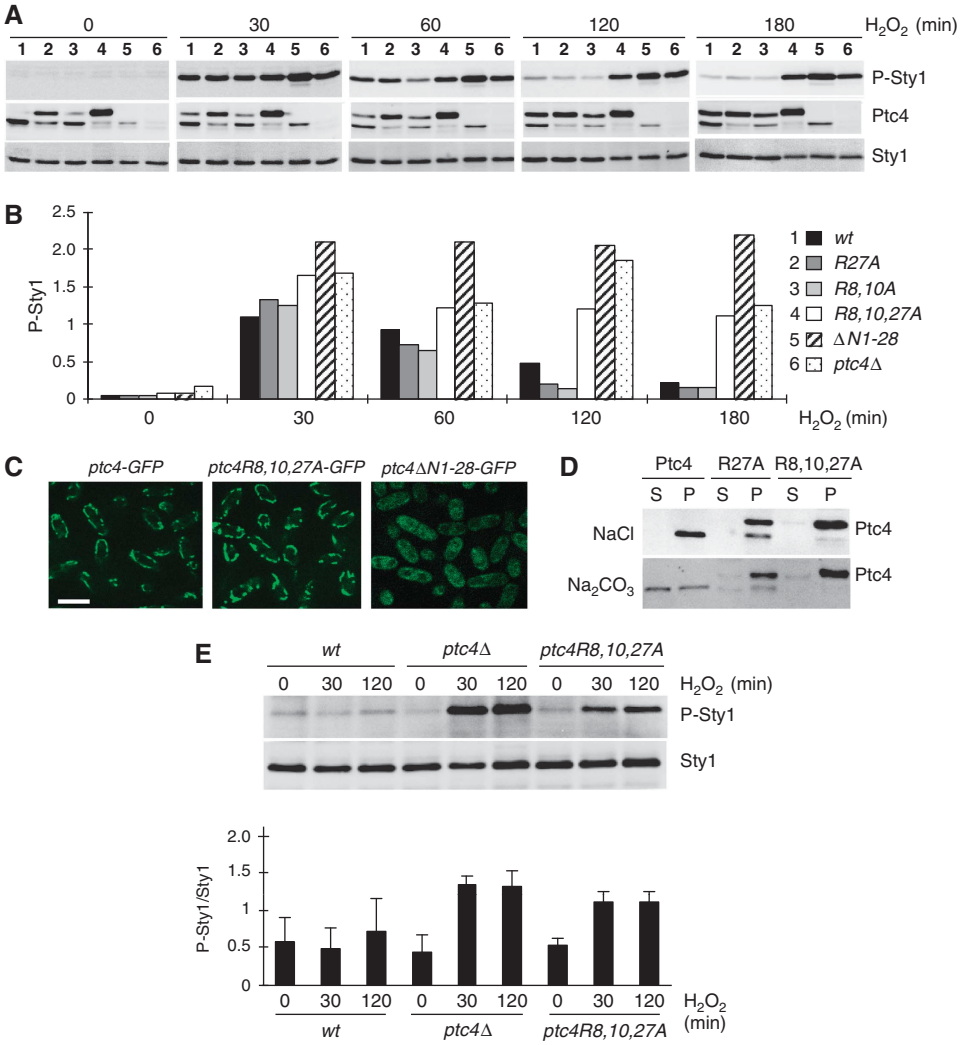

Figure 5 Mutating the MTS of Ptc4 disrupts binding to Sty1 and leads to hyperactivation of the kinase upon oxidative stress. (**A**) Sty1 activation upon H_2O_2 was assessed by immunoblotting extracts prepared from the following strains: 1-*ptc4-3Pk*; 2-*ptc4R27A-3Pk*; 3-*ptc4R8A,R10A-3Pk*; 4-*ptc4R8A,R10A,R27A-3Pk*; 5-*ptc4ΔN1-28-3Pk*; 6-*ptc4Δ*. Results are representative of three independent experiments. (**B**) Quantitation of the levels of Sty1 activation at each time point calculated from (**A**) and corrected for the total amount of Sty1 protein. (**C**) The localization of the indicated forms of Ptc4 was examined by live-cell imaging using immunofluorescence microscopy. The size bar represents 10 μM. *ptc4R8A,R10A,R27A-GFP* indicated by *ptc4R8,10,27A-GFP*. (**D**) Constitutive association of the mutant forms of Ptc4 with mitochondrial membranes. Purified mitochondria from either wild-type (Ptc4) or the *ptc4R27A* and *ptc4R8A,R10A,R27A* mutants were subjected to sodium carbonate treatment as described in Figure 3B. The fractions were assessed by immunoblotting as indicated. S and P represent the supernatant and pellet fractions, respectively. (**E**) Mitochondrial Sty1 is hyperactivated in *ptc4Δ* and in the *ptc4R8,10,27A* mutant. Mitochondria were purified from the indicated strains in the presence or absence of 1 mM H_2O_2. The time points of stress were 30 min and 2 h. The activation status of Sty1 was assessed by immunoblotting. The results are representative of three independent experiments, which have been quantified (P-Sty1/Sty1) and the results are shown in the bottom panel. Figure source data can be found in Supplementary data.

we suggest that a mitochondrial pool of Sty1 is a stress-specific target of this phosphatase: first, Sty1 activation is increased and prolonged in *ptc4Δ*, specifically upon H_2O_2; second, an interaction is observed between endogenous levels of the two proteins; third, a pool of Sty1 is localized to the mitochondria in a similar manner to Ptc4. We believe this is the first evidence to suggest that a mitochondrially localized phosphatase directly regulates a MAPK in this organelle. We propose that Ptc4 regulates the mitochondrial fraction of Sty1 while the remaining intracellular MAPK pool is downregulated by a combination of cytoplasmic phosphatases (Figure 7A), although we cannot exclude that this latter portion of Sty1 shuttles through the mitochondria in addition to its nuclear translocation.

How is the mitochondrial pool of Sty1 activated? There may be a separate MAPK signalling module inside the mitochondria; alternatively, Sty1 might translocate there after prior activation in the cytoplasm. We strongly favour the former idea as first, our data suggest that phosphorylation of Sty1 is not a prerequisite for its mitochondrial entry and second we have observed other components of the Sty1 pathway in mitochondria in cellular fractionation experiments (our unpublished results). Localizing a stress-signalling MAPK module to a compartment responsible for the majority of intracellular ROS production could promote a timely response to oxidative damage. We hypothesize that the fraction of Sty1 localized to the mitochondria contributes to the regulation of this organelle through phosphorylation

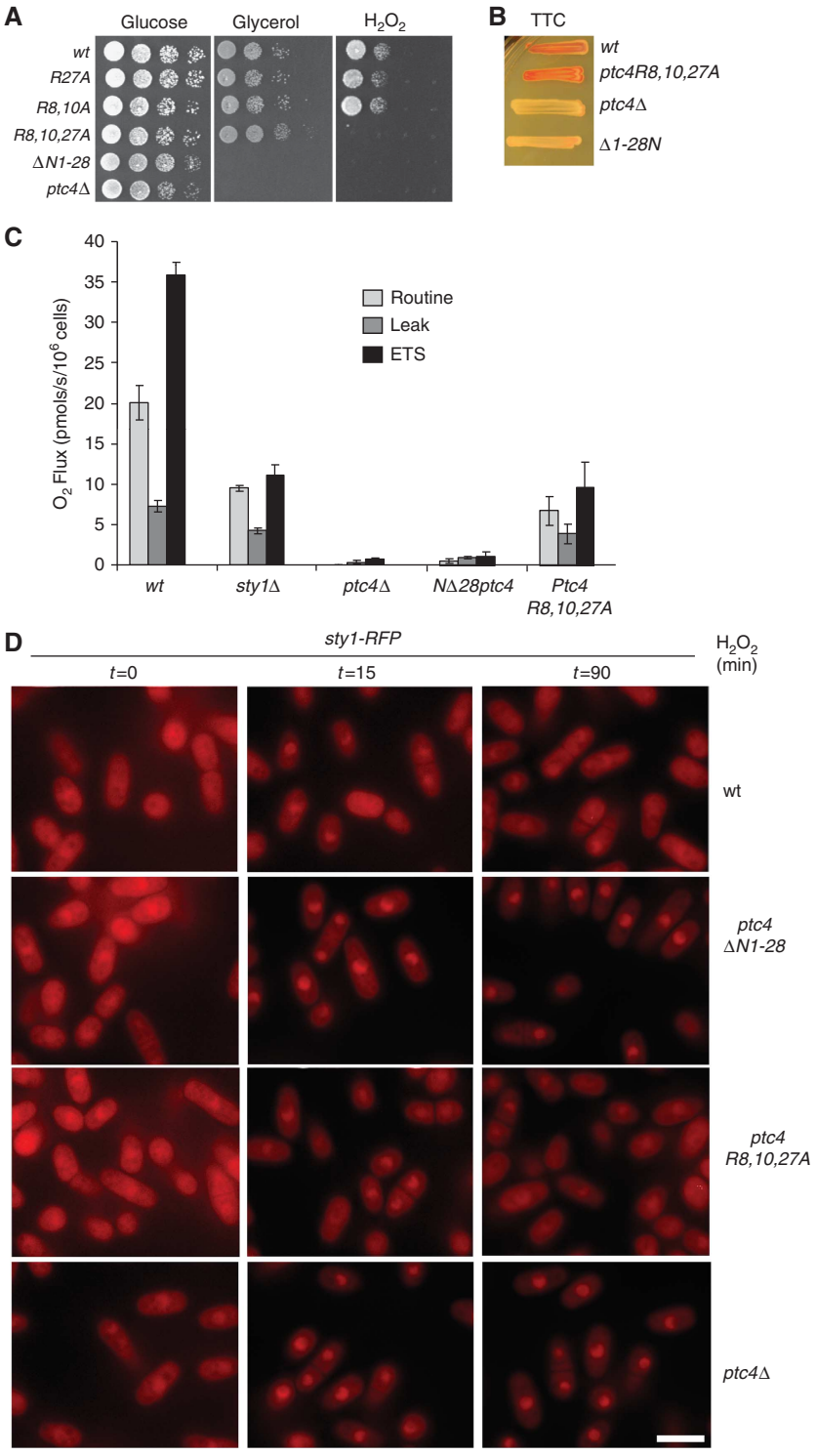

Figure 6 Loss of Ptc4 may affect Sty1 directly through loss of dephosphorylation and also indirectly due to disruption of other mitochondrial functions of Ptc4. (**A**) Increasing dilutions of cells were plated on yeast extract containing either glucose or glycerol as well as YE glucose plates containing 1 mM H_2O_2. Plates were photographed after incubation at 30°C for 5 days. (**B**) Yeast were incubated for 3 days at 30°C on YE containing 1% glucose then overlaid with agar containing 2,3,4-triphenyltetrazolium chloride and incubated for a further 3 h at 30°C. If cells are competent for respiration the colonies turn red, but if not, the colonies remain white (Ogur *et al*, 1957). (**C**) Oxygen consumption was measured from the indicated strains which had been grown in YE overnight and then diluted to 3.5×10^6 cells/ml. The routine level is measured upon placing cells in the respirometer without any drugs. ETS represents the maximum rate of the electron transport system as determined by measuring oxygen consumption upon addition of the proton ionophore FCCP. Upon addition of an ATP synthase inhibitor (TET), protons accumulate on the outside of the inner mitochondrial membrane. Under these conditions, respiration is inhibited and the small amount that does occur, as a result of protons leaking across the inner membrane, is designated 'Leak'. The error bars represent the standard error of three independent experiments. (**D**) The triple R-A mutant of Ptc4 does not result in accumulation of Sty1 in the nucleus for prolonged periods upon oxidative stress. The signal corresponding to Sty1–RFP was assessed by fluorescence microscopy in the indicated strains, which were treated with 1 mM H_2O_2. The scale bar represents 10 μM.

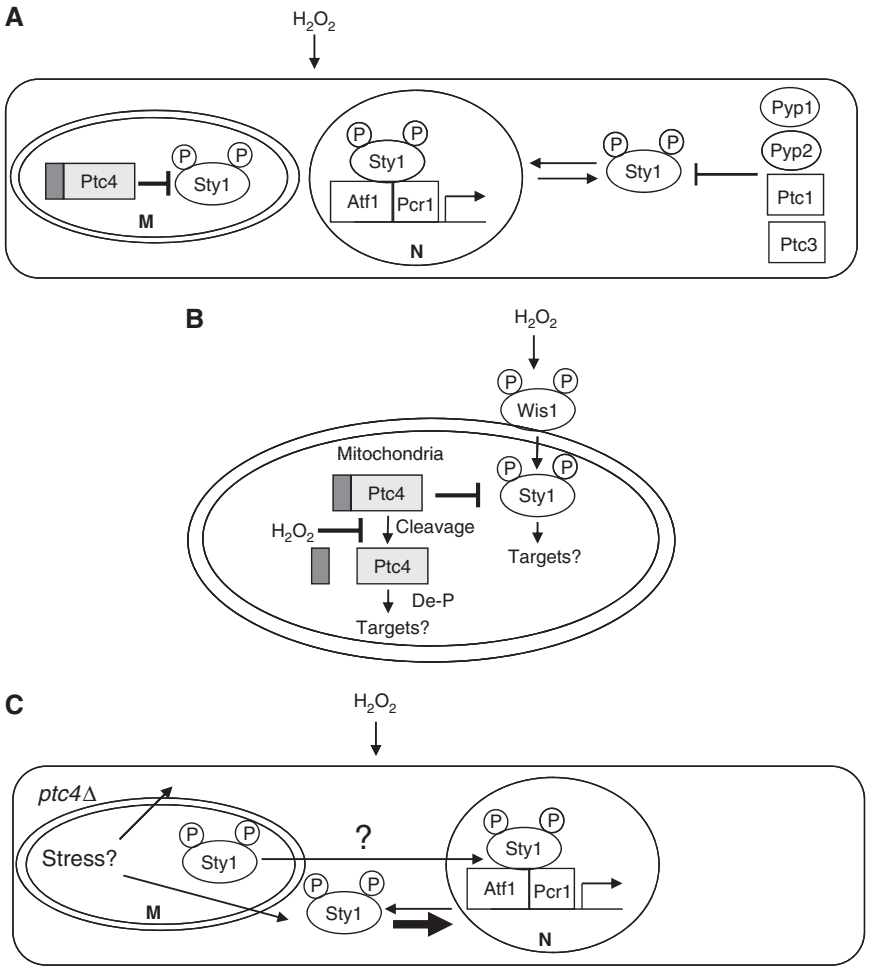

Figure 7 The role of Ptc4 in regulating Sty1 activation upon oxidative stress. See Discussion for details. (**A**) The cytoplasmic pool of Sty1 that shuttles into the nucleus may be downregulated by a combination of several different cytoplasmic phosphatases. M—mitochondria; N—nucleus. (**B**) Ptc4 attenuates activation of a mitochondrial pool of Sty1 upon H_2O_2. De-P indicates that Ptc4 may regulate various aspects of mitochondrial function through the de phosphorylation of mitochondrial proteins. P—a phosphorylated residue. Both Ptc4 and Sty1 have a strong association with the mitochondrial membrane fraction. Retention of the MTS of Ptc4 seems to promote its association with membranes. IM—inner membrane, OM—outer membrane. (**C**) A model for indirect hyperactivation of Sty1 by loss of Ptc4. The cytoplasmic pool of Sty1 could be affected by loss of Ptc4 due to the compromised mitochondrial activities in this mutant resulting in additional stress. This hyperactivated cytoplasmic pool of Sty1 would then translocate into the nucleus.

of targets therein. One possible function is that Sty1 regulates respiration as deletion of *sty1* results in reduced oxygen consumption although further work will be required to determine if this is a result of directly regulating mitochondrial components through phosphorylation. Interestingly, the addition of the uncoupling agent FCCP to *sty1*Δ cells did not result in a significant elevation of oxygen consumption as it does in wild-type cells, suggesting that one defect in this mutant is an uncoupling of the ETC from the proton gradient which is a major respiratory control point (Groen *et al*, 1982).

Our work has uncovered a novel mechanism by which oxidative stress regulates the function of a mitochondrial protein. Exposure to H_2O_2 generates full-length Ptc4 which has greater affinity for Sty1 and promotes association of Ptc4 with the mitochondrial membrane fraction, which is where Sty1 is predominantly located (Figure 7B). Our data suggest that H_2O_2 is affecting a particular mitochondrial function rather than Ptc4 itself as the full-length isoform of Ptc4 can be observed within mitochondria in the *in-vitro* import assays. This isoform may arise due to H_2O_2-specific inhibition of a mitochondrial protease. Ptc4 is cleaved in an MPP-dependent manner during *in-vitro* import assays (Supplementary Figure S9), suggesting that this activity is responsible for cleavage and therefore could be subject to stress-specific regulation. Alternatively, the import of Ptc4 might be affected by oxidation such that it is not correctly localized within the mitochondria for efficient cleavage to occur. Future work will aim to elucidate the mechanism by which H_2O_2 modulates mitochondrial function to give rise to the full-length isoform of Ptc4. We speculate that this regulatory mechanism might apply to other mitochondrial proteins, resulting in oxidative stress-specific isoforms that possess separate functions from their processed counterparts. Indeed, H_2O_2 mildly inhibits cleavage of the Hsp60 MTS (Figure 3D). In the case of Ptc4, its mRNA levels increase dramatically upon H_2O_2 (Chen *et al*, 2003) thus providing a potentially large fraction of newly synthesized, full-length protein under these conditions.

Loss of *ptc4* results in prolonged nuclear accumulation of Sty1 upon oxidative stress; yet, we propose that Ptc4 directly

Table I *S. pombe* strains used in this work

Strain	Genotype	Strain number	Source
Wild type	*h*$^+$ *leu1-32 ura4-D18 his7-366 ade6-M210*	NJ1	Laboratory stock
*ptc4*Δ	*h*$^+$*ptc4*::*natMX6 leu1-32 ura4-D18 his7-366 ade6-M210*	NJ1284	This study
wis1-DD	*h*$^-$ *wis1-DD:ura4*$^+$ *leu1-32 ura4-D18*	NJ892	Shiozaki *et al* (1998)
*wis1-DD ptc4*Δ	*h*$^-$ *wis1-DD:ura4*$^+$ *ptc4*::*natMX6 leu1-32 ura4-D18*	NJ894	This study
*ptc1*Δ *ptc2*Δ *ptc3*Δ	*h*$^-$ *leul-32 ura4-D18 ptcl*::*LEU2 ptc2*::*ura4*$^+$ *ptc3*::*ura4*$^+$	NJ1446	Shiozaki and Russell (1995b)
*pyp2*Δ	*h*$^-$ *pyp2*::*natMX6 leu1-32 ura4-D18 his7-366 ade6-M216*	NJ1113	Laboratory stock
*pyp2*Δ *ptc4* Δ	*h*$^?$*pyp2*::*natMX6 ptc4*::*natMX6 leu1-32 ura4-D18 his7-366 ade6-M210*	NJ1119	This study
*pyp1*Δ	*h*$^+$*pyp1*::*kanMX6 leu1-32 ura4-D18 his7-366 ade6-M210*	NJ102	Laboratory stock
sty1-GFP	*h*$^-$ *sty1-GFP:kanMX6*	NJ952	This study
*sty1-GFPptc4*Δ	*h*$^-$ *sty1-GFP:kanMX6 ptc4*::*natMX6 ura4-D18 ade6-M216*	NJ953	This study
ptc4-3Pk	*h*$^+$*ptc4-3Pk:kanMX6 leu1-32 ura4-D18 his7-366 ade6-M210*	NJ1280	This study
ptc4R27A-3Pk	*h*$^+$ *ptc4-R27A-3Pk:kanMX6 leu1-32 ura4-D18 his7-366 ade6-M210*	NJ1281	This study
ptc4R8A,R10A-3Pk	*h*$^+$ *ptc4R8A,R10A-3Pk leu1-32 ura4-D18 his7-366 ade6-M210*	NJ1603	This study
ptc4R8A,R10A,R27A-3Pk	*h*$^+$*ptc4R8A,R10A,R27A-3Pk leu1-32 ura4-D18 his7-366 ade6-M210*	NJ1583	This study
*ptc4*Δ*N1-28-3Pk*	*h*$^+$*ptc4*Δ*N1-28-3Pk leu1-32 ura4-D18 his7-366 ade6-M210*	NJ1283	This study
cox4-GFP ptc4-RFP	*h*$^+$*cox4-GFP:kanMX6 ptc4-RFP:hygMX6 leu1-32 ura4-D18 his7-366 ade6-M210*	NJ1040	This study
ptc4-GFP sty1-RFP	*h*$^+$*ptc4-GFP:kanMX6 sty1-RFP:hygMX6 leu1-32 ura4-D18 his7-366 ade6-M210*	NJ1290	This study
sty1-RFP ptc4-GFP	*h*$^+$*sty1-RFP(tom):hygMX6 ptc4-GFP leu1-32 ura4-D18 his7-366 ade6-M210*	NJ1290	This study
*sty1-RFP ptc4*Δ	*h*$^+$*ptc4*::*natMX6 sty1-RFP(tom):hygMX6 leu1-32 ura4-D18 his7-366 ade6-M210*	NJ1288	This study
*sty1-RFP ptc4*Δ*N1-28-GFP*	*h*$^+$*ptc4*Δ*N1-28 sty1-RFP(tom):hygMX6 leu1-32 ura4D18 his7-366 ade6-M210*	NJ1294	This study
sty1-RFP ptc4R8A,R10A,R27-GFP	*h*$^+$*ptc4R8A,R10A,R27A sty1-RFP(tom):hygMX6 leu1-32 ura4-D18 his7-366 ade6-M210*	NJ1292	This study

dephosphorylates a mitochondrial pool of Sty1. How can these two observations be reconciled? Perhaps upon prolonged H_2O_2, Sty1 may exit the mitochondria. In *ptc4*Δ, the pool of Sty1 entering the cytoplasm would still be activated and therefore potentially translocated to the nucleus. In this way, Sty1 could communicate the status of the mitochondria to the rest of the cell to influence further responses to prolonged stress. Alternatively, as loss of Ptc4 leads to defects in oxidative phosphorylation, this could result in an increase in cellular stress such as ROS, which in combination with prolonged exogenous ROS exposure, could result in hyperactivation of the cytoplasmic pool of Sty1, again leading to its nuclear accumulation. The increase in Sty1 activation observed in *ptc4*Δ could be a combination of this indirect effect, leading to activation of the cytoplasmic pool of Sty1, coupled with loss of direct dephosphorylation of mitochondrial Sty1 (Figure 7C). In the triple arginine mutant, mitochondrial Sty1 is hyperactivated but nuclear accumulation of Sty1 is not as prolonged, suggesting that the indirect effect due to loss of Ptc4 activity in this mutant is not as pronounced as in *ptc4*Δ. Consistent with this, although the triple mutant has a reduced respiratory capacity, it is not as compromised as the delete and can respire sufficiently to support growth on glycerol.

Future work will aim to elucidate how Ptc4 and Sty1 regulate mitochondrial function and to determine the mechanisms by which oxidative stress influences cleavage of the phosphatase and activates mitochondrial Sty1.

Materials and methods

Yeast strains and general methods

The strains of *S. pombe* used in this study are listed in Table I. Yeast media and general methods were as described (Moreno *et al*, 1991). Unless otherwise stated, all cells were grown to mid-log phase in yeast extract at 30°C. Gene deletions and epitope tagging were carried out as described (Bähler *et al*, 1998). Integrating gene mutations into genomic DNA with the Cre-loxP system was as described (Iwaki and Takegawa, 2004). All oligonucleotide sequences used in this study are available upon request. All epitope-tagged *ptc4* strains were assessed for their ability to grow on minimal media or YE containing glycerol as a carbon source and were found to grow at the same rate as wild type in contrast to the *ptc4* delete mutant, which displayed a growth defect under these conditions. This suggested that the tags did not significantly affect Ptc4 function. Cells were harvested by filtration.

Protein extraction and western blotting

Native *S. pombe* cell extracts were prepared by glass bead lysis in the following buffer (50 mM HEPES pH7.5, 150 mM NaCl, 50 mM NaF, 40 mM glycerophosphate, 0.2 mM sodium vanadate, 1 mM PMSF, 0.5% NP-40, protein inhibitor complete™). Before lysis, cells were washed once in stop buffer (10 mM EDTA, 1 mM NaN_3, 0.01% NaCl, 50 mM NaF, 1 mM sodium vanadate). Protein extracts were separated by SDS–polyacrylamide gel electrophoresis and transferred onto nitrocellulose. Antibodies used were anti-phospho-p38 (Genway), anti-Hog1 (Santa Cruz), anti-Pk (Serotec), anti-Hsp60 (Sigma), anti-Cox2 (a kind gift from Nathalie Bonnefoy), anti-Rpb1 (Covance) and anti-Tpx1 (a kind gift from Elizabeth Veal). Activated Sty1 was detected using anti-phospho-p38 antiserum, which recognizes the dually phosphorylated activation site of pTGpY (P-Sty1). Total Sty1 levels (Sty1) were assessed using antiserum raised against Hog1, the *S. cerevisiae* homologue of Sty1. Quantification of western blot signals was performed using the chemi Genius Bioimaging system (Syngene). For all analyses using *ptc4* mutants, freshly constructed or freshly re-isolated strains were used.

Fluorescence microscopy

For all live-cell imaging, cells were mounted in a Biopatchs FC2 chamber with lectin (Sigma, L2380; 0.05 mg/ml). For live imaging on the Deltavision Spectris system, 0.1 μm consecutive slices were continuously captured with a single passage through a set of 10 slices. Cells were grown in filter-sterilized EMM supplemented media (Moreno *et al*, 1991). All imaging analysis used Imaris (Bitplane) software (Grallert *et al*, 2004).

Electron microscopy

Mitochondria were purified as described (Chiron *et al*, 2007) and fixed in 4% formaldehyde in SEM buffer (250 mM sucrose, 1 mM EDTA, 10 mM MOPS-KOH, pH 7.2) for 1 h at room temperature. The fixed samples were embedded with gelatine, then cryoprotected with 2.3 M sucrose, then frozen and cut at −120°C. The sections were thawed, labelled with anti-Myc antibodies (Santa Cruz 789) and protein-A conjugated with 15 nm gold particles (British Biocell) and embedded with a methylcellulose/uranyl acetate mix as described (Liou *et al*, 1996).

Subcellular fractionation

Purification of mitochondria, submitochondrial fractionation procedures fraction and Proteinase K treatment methods were as described (Chiron *et al*, 2007). These procedures were carried out using the *ptc4-3Pk* strain; Ptc4 was monitored via immunoblotting using anti-Pk antiserum. Mitochondrial fractions were treated with 1.25, 2.5 or 5 μg/ml for 30 min as indicated by the black triangles in Figure 3D. Further purification of mitochondria by centrifugation through a sucrose gradient was as described (Meisinger *et al*, 2006). Mitoplasts were prepared from purified mitochondria by treatment in hypotonic buffer (0.06 M sorbitol, 20 mM HEPES-KOH pH 7.4, 2 mM EDTA) as described (Boldogh and Pon, 2007). In Figure 3D, 'total' represents intact mitochondria; 'swollen' represents mitochondria treated with hypotonic buffer to rupture the outer membrane and release the contents of the inner membrane space; 'sonicated' represents the resulting mitoplasts that have been sonicated in the presence of salt which will disrupt the inner membrane to release the matrix contents. Carbonate treatment was as described (Boldogh and Pon, 2007). For fractionation experiments to examine Sty1 phosphorylation, the following phosphatase inhibitor cocktails were added to lysis buffer at a dilution factor of 1 in 1000: Sigma P5726 and P0044.

Identification of the mature N-terminus of Ptc4

The strain NJ1280 carrying the ORF of *ptc4* fused with three copies of the Pk epitope at its carboxy-terminus was ground in the presence of liquid nitrogen with a SPEX SamplePrep LLC 6850 freezer/mill, and suspended in lysis buffer (50 mM HEPES pH 7.5, 150 mM NaCl, 50 mM NaF, 40 mM glycerophosphate, 0.2 mM sodium vanadate, 1 mM PMSF, 0.5% NP-40, protein inhibitor complete). Ptc4-3Pk protein was isolated by immunoprecipitation with magnetic Dynabeads IgG (Invitrogen) conjugated with mouse anti-V5 (Sigma S-1265) at 4°C. The beads were washed six times in lysis buffer and boiled for 10 min in SDS buffer. The resulting Ptc4 protein was analysed by Edman degradation by TOPLAB GmbH, Martinsried, Germany.

Import assays

These were carried out as described (Bender *et al*, 2010) except that 150 μg/ml of proteinase K was used for 20 min. GST-Ptc4-Pk (three copies of the Pk tag) was expressed in *E. coli*, and the resulting fusion protein was purified on GSH-Sepharose beads followed by treatment with thrombin to release Ptc4-3Pk.

Co-immunoprecipitation and in-vitro binding assays

For immunoprecipitation analysis, cells were obtained by filtration from exponentially growing cultures. The IP lysis buffer and IP method were as described (Nguyen *et al*, 2002). The protein extract was incubated with 10 μl anti-V5 agarose (Sigma) for 3 h at 4°C. Wild-type and mutant forms of Ptc4-3Pk were generated using an original TNT-coupled Reticulocyte lysate system and the resulting proteins were incubated with GST–Sty1 or GST for 3 h at 4°C. GST and GST–Sty1 were expressed in *E. coli* and purified on GSH-Sepharose beads (GE Healthcare). The beads were washed four times in IP buffer and bound proteins eluted by boiling for 10 min in SDS sample buffer. Ptc4-Pk was detected using anti-Pk antiserum.

The binding efficiency between *in vitro* translated Ptc4 and GST–Sty1 was calculated as follows: the levels of GST–Sty1 were compared between each sample. This was used to correct the amount of Ptc4 bound in each case. The amounts of each isoform of Ptc4 bound were then corrected for the total amounts present in the input.

Dilution assays

These were carried out as described (Lawrence *et al*, 2007). YE plates containing either 3% glycerol instead of glucose were used to assess respiratory competence.

Respiration assays (TTC)

These were carried out as described (Ogur *et al*, 1957).

Site-directed mutagenesis

This was carried out using the QuikChange kit (Stratagene) according to the manufacturer's instructions.

High-resolution respirometry

This was performed as described (Leadsham and Gourlay, 2010) except that the following drug concentrations were used: TET 400 μM; FCCP 48 μM and antimycin A 2 μM. All drugs were from Sigma. The addition of antimycin A enabled the calculation of non-mitochondrial oxygen consumption, which was found to be undetectable. Cells were grown overnight in YE and diluted to 3.5×10^6/ml in fresh YE before placing in the chamber.

Supplementary data

Supplementary data are available at *The EMBO Journal* Online (http://www.embojournal.org).

Acknowledgements

We thank Claire Rooney for help with the early stages of this project; Nathalie Bonnefoy and Elizabeth Veal for helpful advice and reagents; Paul Russell and Jonathan Millar for strains and John Armstrong; Elizabeth Veal and Steve Lyons for critical comments on the manuscript. This work was funded by Cancer Research UK including a Cancer Research UK—China Fellows Programme award to YD.

Author contributions: YD performed most of the experiments with contributions from AB, KD and CW. EH, VK and CG performed and analysed the respirometry. AM performed the electron microscopy. CW wrote the manuscript with significant input from YD and NJ. Experiments were conceived and analysed by YD, CW and NJ.

Conflict of interest

The authors declare that they have no conflict of interest.

References

Bähler J, Wu JQ, Longtine MS, Shah NG, McKenzie III A, Steever AB, Wach A, Philippsen P, Pringle JR (1998) Heterologous modules for efficient and versatile PCR-based gene targeting in Schizosaccharomyces pombe. *Yeast* **14:** 943–951

Bender T, Leidhold C, Ruppert T, Franken S, Voos W (2010) The role of protein quality control in mitochondrial protein homeostasis under oxidative stress. *Proteomics* **10:** 1426–1443

Boldogh IR, Pon LA (2007) Purification and subfractionation of mitochondria from the yeast Saccharomyces cerevisiae. *Methods Cell Biol* **80:** 45–64

Chen D, Toone WM, Mata J, Lyne R, Burns G, Kivinen K, Brazma A, Jones N, Bahler J (2003) Global transcriptional responses of fission yeast to environmental stress. *Mol Biol Cell* **14:** 214–229

Chiron S, Gaisne M, Guillou E, Belenguer P, Clark-Walker GD, Bonnefoy N (2007) Studying mitochondria in an attractive model: Schizosaccharomyces pombe. *Methods Mol Biol* **372:** 91–105

Claros MG, Vincens P (1996) Computational method to predict mitochondrially imported proteins and their targeting sequences. *Eur J Biochem* **241:** 779–786

Gaits F, Degols G, Shiozaki K, Russell P (1998) Phosphorylation and association with the transcription factor Atf1 regulate localization of Spc1/Sty1 stress-activated kinase in fission yeast. *Genes Dev* **12:** 1464–1473

Gaits F, Russell P (1999) Vacuole fusion regulated by protein phosphatase 2C in fission yeast. *Mol Biol Cell* **10:** 2647–2654

Gaits F, Shiozaki K, Russell P (1997) Protein phosphatase 2C acts independently of stress-activated kinase cascade to regulate the stress response in fission yeast. *J Biol Chem* **272:** 17873–17879

Grallert A, Krapp A, Bagley S, Simanis V, Hagan IM (2004) Recruitment of NIMA kinase shows that maturation of the S. pombe spindle-pole body occurs over consecutive cell cycles and reveals a role for NIMA in modulating SIN activity. *Genes Dev* **18:** 1007–1021

Groen AK, Wanders RJ, Westerhoff HV, van der Meer R, Tager JM (1982) Quantification of the contribution of various steps to the control of mitochondrial respiration. *J Biol Chem* **257:** 2754–2757

Habib SJ, Neupert W, Rapaport D (2007) Analysis and prediction of mitochondrial targeting signals. *Methods Cell Biol* **80:** 761–781

Hendrick JP, Hodges PE, Rosenberg LE (1989) Survey of amino-terminal proteolytic cleavage sites in mitochondrial precursor proteins: leader peptides cleaved by two matrix proteases share a three-amino acid motif. *Proc Natl Acad Sci USA* **86:** 4056–4060

Iwaki T, Takegawa K (2004) A set of loxP marker cassettes for Cre-mediated multiple gene disruption in Schizosaccharomyces pombe. *Biosci Biotechnol Biochem* **68:** 545–550

Juneau K, Nislow C, Davis RW (2009) Alternative splicing of PTC7 in Saccharomyces cerevisiae determines protein localization. *Genetics* **183:** 185–194

Kato Jr T, Okazaki K, Murakami H, Stettler S, Fantes PA, Okayama H (1996) Stress signal, mediated by a Hog1-like MAP kinase, controls sexual development in fission yeast. *FEBS Lett* **378:** 207–212

Krause-Buchholz U, Gey U, Wunschmann J, Becker S, Rodel G (2006) YIL042c and YOR090c encode the kinase and phosphatase of the Saccharomyces cerevisiae pyruvate dehydrogenase complex. *FEBS Lett* **580:** 2553–2560

Kyriakis JM, Avruch J (2001) Mammalian mitogen-activated protein kinase signal transduction pathways activated by stress and inflammation. *Physiol Rev* **81:** 807–869

Lawrence CL, Maekawa H, Worthington JL, Reiter W, Wilkinson CR, Jones N (2007) Regulation of Schizosaccharomyces pombe Atf1 protein levels by Sty1-mediated phosphorylation and heterodimerization with Pcr1. *J Biol Chem* **282:** 5160–5170

Leadsham JE, Gourlay CW (2010) cAMP/PKA signaling balances respiratory activity with mitochondria dependent apoptosis via transcriptional regulation. *BMC Cell Biol* **11:** 92

Liou W, Geuze HJ, Slot JW (1996) Improving structural integrity of cryosections for immunogold labeling. *Histochem Cell Biol* **106:** 41–58

Lu G, Ren S, Korge P, Choi J, Dong Y, Weiss J, Koehler C, Chen JN, Wang Y (2007) A novel mitochondrial matrix serine/threonine protein phosphatase regulates the mitochondria permeability transition pore and is essential for cellular survival and development. *Genes Dev* **21:** 784–796

Meisinger C, Pfanner N, Truscott KN (2006) Isolation of yeast mitochondria. *Methods Mol Biol* **313:** 33–39

Millar JB, Buck V, Wilkinson MG (1995) Pyp1 and Pyp2 PTPases dephosphorylate an osmosensing MAP kinase controlling cell size at division in fission yeast. *Genes Dev* **9:** 2117–2130

Moreno S, Klar A, Nurse P (1991) Molecular genetic analysis of fission yeast Schizosaccharomyces pombe. *Methods Enzymol* **194:** 795–823

Nguyen AN, Ikner AD, Shiozaki M, Warren SM, Shiozaki K (2002) Cytoplasmic localization of Wis1 MAPKK by nuclear export signal is important for nuclear targeting of Spc1/Sty1 MAPK in fission yeast. *Mol Biol Cell* **13:** 2651–2663

Nguyen AN, Shiozaki K (1999) Heat-shock-induced activation of stress MAP kinase is regulated by threonine- and tyrosine-specific phosphatases. *Genes Dev* **13:** 1653–1663

Ogur M, St John R, Nagai S (1957) Tetrazolium overlay technique for population studies of respiration deficiency in yeast. *Science* **125:** 928–929

Payne DM, Rossomando AJ, Martino P, Erickson AK, Her JH, Shabanowitz J, Hunt DF, Weber MJ, Sturgill TW (1991) Identification of the regulatory phosphorylation sites in pp42/mitogen-activated protein kinase (MAP kinase). *EMBO J* **10:** 885–892

Petersen J, Hagan IM (2005) Polo kinase links the stress pathway to cell cycle control and tip growth in fission yeast. *Nature* **435:** 507–512

Petersen J, Nurse P (2007) TOR signalling regulates mitotic commitment through the stress MAP kinase pathway and the Polo and Cdc2 kinases. *Nat Cell Biol* **9:** 1263–1272

Pletjushkina OY, Lyamzaev KG, Popova EN, Nepryakhina OK, Ivanova OY, Domnina LV, Chernyak BV, Skulachev VP (2006) Effect of oxidative stress on dynamics of mitochondrial reticulum. *Biochim Biophys Acta* **1757:** 518–524

Robbins DJ, Zhen E, Owaki H, Vanderbilt CA, Ebert D, Geppert TD, Cobb MH (1993) Regulation and properties of extracellular signal-regulated protein kinases 1 and 2 *in vitro*. *J Biol Chem* **268:** 5097–5106

Sharrocks AD, Yang SH, Galanis A (2000) Docking domains and substrate-specificity determination for MAP kinases. *Trends Biochem Sci* **25:** 448–453

Shiozaki K, Russell P (1995a) Cell-cycle control linked to extracellular environment by MAP kinase pathway in fission yeast. *Nature* **378:** 739–743

Shiozaki K, Russell P (1995b) Counteractive roles of protein phosphatase 2C (PP2C) and a MAP kinase kinase homolog in the osmoregulation of fission yeast. *EMBO J* **14:** 492–502

Shiozaki K, Shiozaki M, Russell P (1998) Heat stress activates fission yeast Spc1/StyI MAPK by a MEKK-independent mechanism. *Mol Biol Cell* **9:** 1339–1349

Tal R, Winter G, Ecker N, Klionsky DJ, Abeliovich H (2007) Aup1p, a yeast mitochondrial protein phosphatase homolog, is required for efficient stationary phase mitophagy and cell survival. *J Biol Chem* **282:** 5617–5624

Thorpe GW, Fong CS, Alic N, Higgins VJ, Dawes IW (2004) Cells have distinct mechanisms to maintain protection against different reactive oxygen species: oxidative-stress-response genes. *Proc Natl Acad Sci USA* **101:** 6564–6569

Wilkinson MG, Samuels M, Takeda T, Toone WM, Shieh JC, Toda T, Millar JB, Jones N (1996) The Atf1 transcription factor is a target for the Sty1 stress-activated MAP kinase pathway in fission yeast. *Genes Dev* **10:** 2289–2301

Zuin A, Gabrielli N, Calvo IA, Garcia-Santamarina S, Hoe KL, Kim DU, Park HO, Hayles J, Ayte J, Hidalgo E (2008) Mitochondrial dysfunction increases oxidative stress and decreases chronological life span in fission yeast. *PLoS One* **3:** e2842